doi.org/10.26434/chemrxiv.9733628.v2

Rationalizing the diverse reactivity of [1.1.1]propellane through sigma-pi-delocalization

Alistair Sterling, Alexander Durr, Russell C. Smith, Edward Anderson, Fernanda Duarte

Submitted date: 05/02/2020 • Posted date: 07/02/2020

Citation information: Sterling, Alistair; Durr, Alexander; Smith, Russell C.; Anderson, Edward; Duarte, Fernanda (2019): Rationalizing the diverse reactivity of [1.1.1]propellane through sigma-pi-delocalization. ChemRxiv. Preprint. https://doi.org/10.26434/chemrxiv.9733628.v2

[1.1.1]Propellane has gained increased attention due to its utility as a precursor to bicyclo[1.1.1]pentanes (BCPs) – motifs of high value in pharmaceutical and materials research – by addition of nucleophiles, radicals and electrophiles across its inter-bridgehead C–C bond. However, the origin of this broad reactivity profile is not well-understood. Here, we present a comprehensive computational study that attributes the omniphilicity of [1.1.1]propellane to a moldable, delocalized electron density, characterized by the mixing of the inter-bridgehead C–C bonding and antibonding orbitals. Reactions with anions and radicals are facilitated by stabilization of the adducts through sigma-pi-delocalization of electron density over the cage, while reactions with cations involve charge transfer that relieves Pauli repulsion inside the cage. These results provide a unified framework to rationalize propellane reactivity, opening up opportunities for the exploration of new chemistry of [1.1.1]propellane and related strained systems.

Rationalizing the diverse reactivity of [1.1.1]propellane through σ-π-delocalization

Alistair J. Sterling,[a] Alexander B. Dürr,[a] Russell C. Smith,[b] Edward A. Anderson[a]* and Fernanda Duarte[a]*

Abstract: [1.1.1]Propellane has gained increased attention due to its utility as a precursor to bicyclo[1.1.1]pentanes (BCPs) – motifs of high value in pharmaceutical and materials research – by addition of nucleophiles, radicals and electrophiles across its inter-bridgehead C–C bond. However, the origin of this broad reactivity profile is not well-understood. Here, we present a comprehensive computational study that attributes the omniphilicity of [1.1.1]propellane to a moldable, delocalized electron density, characterized by the mixing of the inter-bridgehead C–C bonding and antibonding orbitals. Reactions with anions and radicals are facilitated by stabilization of the adducts through σ-π-delocalization of electron density over the cage, while reactions with cations involve charge transfer that relieves Pauli repulsion inside the cage. These results provide a unified framework to rationalize propellane reactivity, opening up opportunities for the exploration of new chemistry of [1.1.1]propellane and related strained systems.

Introduction

In recent years, [1.1.1]propellane (**1**, Figure 1) has become a valuable precursor to bicyclo[1.1.1]pentanes (BCPs),[1,2] motifs that are attractive bioisosteres for aryl,[3–8] alkynyl[9] and *tert*-butyl[10] groups in medicinal chemistry due to the enhanced pharmacokinetic profile of the BCP spacer unit compared to the parent motif (Figure 1a). BCPs are also useful motifs for organic materials, including rod-like one-dimensional polymers,[11] supramolecular spacer units,[12] liquid crystals[13] and FRET sensors.[14] Such applications have stimulated the development of a number of methods to access BCPs in a single step from **1**, via radical[15–20] and anionic[21–25] intermediates (Figure 1b). Limitations nonetheless remain, in particular due to the surprisingly harsh reaction conditions often required for these processes, which can restrict functional group tolerance. A third reactivity mode of **1** involves cationic addition, which generates a bicyclo[1.1.1]pentyl cation that rapidly fragments to an *exo*-methylenecyclobutane.[26]

This diverse 'omniphilic' reactivity profile has traditionally been ascribed to the high strain energy of [1.1.1]propellane (total strain energy = ~100 kcal mol^{-1}),[27] albeit only ~30 kcal mol^{-1} of this ring strain is predicted to be released on

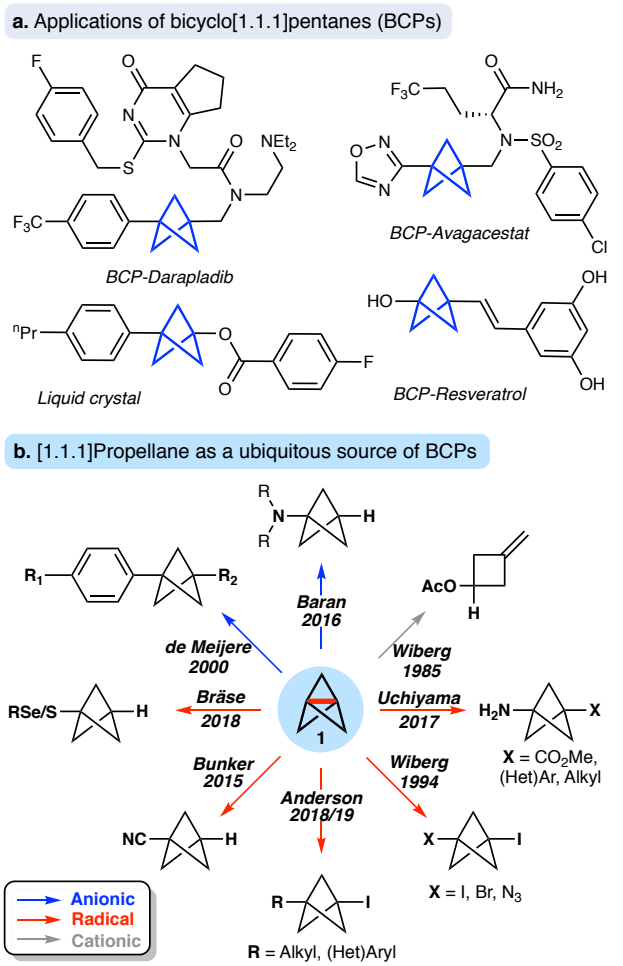

Figure 1. a. Applications of bicyclo[1.1.1]pentanes (BCPs) in pharmaceutical and materials settings. **b.** The omniphilic reactivity of [1.1.1]propellane with anions / organometallics (blue arrows), radicals (red arrows) and cations (gray arrows).

cleavage of the inter-bridgehead C1–C3 bond.[2,28] Although similar to the strain energy of cyclopropane (~28 kcal mol^{-1}), it is notable that the latter does not display the same broad spectrum of reactivity.[29] Moreover, in contrast to standard S_N2 reactions, the inverted geometry of the bridgehead carbon atom in **1** circumvents the need for planarization in the transition state,[30] which might suggest that activation barriers arise from a change in electronic structure, rather than through relief of ring strain alone, as is generally supposed.[22,27] To date, a handful of experimental studies have employed density functional theory (DFT) to investigate the pathways of addition of radicals and anions to [1.1.1]propellane, offering valuable insight to support reaction development.[15–17,24,25] However, no in-depth theoretical analysis has tackled the origin of the omniphilic reactivity of **1**.

In this work, we combine *ab initio* approaches with Electron Density Difference Analysis (EDDA) and Distortion/Interaction Analysis (DIA)[30–32] to develop a unified model for the reactivity of [1.1.1]propellane. Contrary to classical explanations, we demonstrate that its chemistry is not determined simply by geometric 'strain relief'; instead, it is the change in electron delocalization over the cage that defines the observed activation profiles. These results bridge the gap between the theoretical understanding of [1.1.1]propellane as a 'scientific curiosity' to its applications in real-life settings.[2]

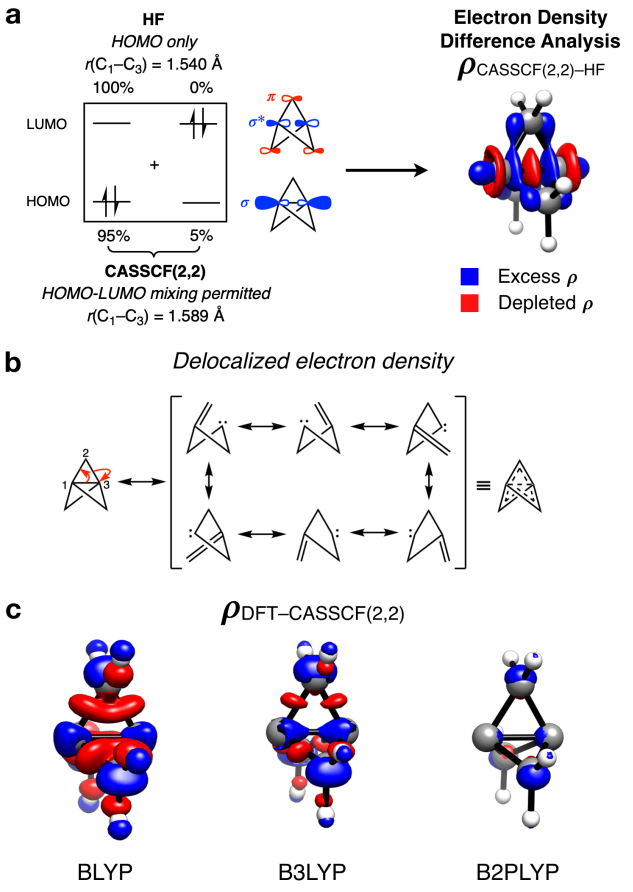

Figure 2. a. Left: MOs in the (2,2) active space with their corresponding atomic orbital composition and population. **Right:** [CASSCF(2,2)]–[RHF] electron density difference plot for **1**, isovalue = 0.002 a.u. **b.** Resonance forms of the Lewis structure of **1** showing sacrificial hyperconjugation (blue box), which results in a delocalized electron density. **c.** DFT electron density difference plot for **1**: [BLYP]–[CASSCF(2,2)] (left), [BLYP]–[CASSCF(2,2)] (center), [B2PLYP]–[CASSCF(2,2)] (right); isovalue of 0.01 a.u. Geometry optimized at CASSCF(2,2). All calculations use the def2-QZVPP basis set.

Results and Discussion

The structure of [1.1.1]propellane

Before considering the reactivity of [1.1.1]propellane, we first sought to characterize the nature of the inter-bridgehead C1– C3 bond in the ground state (Figure 2a). The geometry of **1** has been determined experimentally by low-temperature X-ray diffraction[33] and gas-phase electron diffraction;[34] from the latter, the C1–C3 distance was found to be 1.594 Å which, being similar to the C–C bond length in ethane (1.524 Å),[35] is suggestive of a C1–C3 bonding interaction. The nature of this bonding has been much debated over the past 30 years, with both theoretical[36,37,46,47,38–45] and experimental[26,34,36,48–51] studies offering contrasting evidence. For example, despite a closed-shell singlet ground state and a calculated bond energy of ~65 kcal mol^{-1},[36] photoelectron spectroscopy reveals the HOMO (C1–C3 σ-bonding) to be non-bonding due to poor orbital overlap between the 'inverted' carbons.[51] This

result is corroborated by synchrotron experiments that reveal depletion of electron density at the bond critical point.[49]

Such studies led to the proposal that the inverted C1–C3 bond in **1** should be best described as a charge-shift bond, with its stability attributed to resonance stabilization between the covalent ([C1•---•C3], repulsive) and ionic ([C1:$^{(-)}$---$^{(+)}$C3] and [C1$^{(+)}$---$^{(-)}$:C3], attractive) structures.[47] This type of bonding arises through significant Pauli repulsion pressure[52,§] between each of the C1/3–C2 'wing' bonds and the C1–C3 bond,[53] and accounts for both the observed closed-shell singlet ground state and the unusual positive sign of the Laplacian of the electron density at the critical point of the C1–C3 bond. However, the consequences of the unique electronic configuration of **1** on its reactivity remains an open question.

To further quantify the effects of the electronic repulsion within the propellane cage, the complete active space (CASSCF) method was used (with a (2,2) active space, for the formal inclusion of static correlation), which allows electrons to populate both the HOMO (C–C σ-bonding) and LUMO (C–C σ-antibonding) (Figure 2a). In 'normal' closed-shell organic molecules, >1.98 electrons populate the HOMO, however in **1** we found this value to be 1.91 electrons, indicating that static correlation effects are important. Such behavior is typically only seen in systems with near-degenerate frontier orbitals, which is certainly not the case here (E_{gap} = 13.0 eV). We propose that significant HOMO-LUMO mixing is capable of reducing the unusually high electronic repulsion inside the propellane cage. The effect of this mixing can be seen in the stabilization of the structure of **1** by 19.2 kcal mol^{-1}, with an increase in the calculated C1–C3 bond distance from 1.540 to 1.589 Å (def2-QZVPP basis set), which is in excellent agreement with experiment.

An electron density difference plot (Figure 2a) comparing the Hartree-Fock (HOMO-only) and CASSCF(2,2) (HOMO-LUMO mixing) densities revealed that charge is depleted from the center of the cage (red lobes), and is instead delocalized onto the bridging carbon atoms (blue lobes). This correlates well with the depleted electron density observed at the critical point of the C1–C3 bond. This electronic reorganization can be considered as 'σ-π-delocalization' (σ→[σ*+ π]), where the σ-antibonding orbital of the LUMO is of the correct symmetry to overlap with π orbital formed from p orbitals on the bridging carbon atoms. This effect can also be represented in terms of resonance forms (Figure 2b), where the C1–C3 bond breaks to form six degenerate alkene/carbene pairs. To our knowledge, this is the only example of stabilization of a neutral hydrocarbon through 'sacrificial hyperconjugation' (where the resonance structure contains one two-electron bond less than the Lewis representation).[54] Overall, this description of the electronic structure of **1** is equivalent to the 'charge-shift' model introduced by Shaik and co-workers,[47] but has the advantage of enabling the exploration of the effects of delocalization on reactivity.

Modelling the reactivity of **1** using density functional theory (DFT) is challenging due to the static correlation effects mentioned above. The performance of DFT depends directly on the electron density, and the challenge in the context of **1** arises from low density in the C1–C3 region.[55] This problem can be qualitatively depicted using density difference plots (Figure 2c), which were calculated for a range of DFT functionals and compared to those obtained with CASSCF(2,2). Interestingly, the GGA functional (BLYP)[56,57] accurately predicts the C1–C3 bond length to <0.01 Å; however, it poorly reproduces the CASSCF(2,2) density, and substantially over-delocalizes electron density across the cage. This is an error that is known for GGA functionals, highlighting the risk of obtaining the 'right answer for the wrong reason'. The incorporation of some exact exchange into the functional

(B3LYP)[58] now over-localizes electron density along the C1–C3 axis, resulting in a bond that is too short, and likely too strong. Pleasingly, further augmentation of the functional through the inclusion of MP2-like correlation (B2PLYP)[59] results in a lengthened C1–C3 bond, and a better match with the CASSCF(2,2) electron density. Further analysis of the singlet-triplet gap and vertical ionization potential for each of these functionals revealed B2PLYP to give the best performance, which we ascribe to a more accurate description of the HOMO-LUMO mixing through the inclusion of explicit correlation (Figure S11).

In light of these results, we considered that a computational methodology capable of describing delocalization and correlation effects would be required to accurately describe the reactivity of [1.1.1]propellane with anions, radicals and cations. A benchmark study of these reactions also revealed that double-hybrid DFT was required to accurately describe the geometric and electronic features of this system (see Supplementary Figures S15-20). Among the double-hybrid functionals tested, B2GP-PLYP-D3BJ with the triple-ζ quality basis set def2-TZVP was found to afford good geometries and energies within 1 kcal mol^{-1} of the reference coupled-cluster method DLPNO-CCSD(T).[60–62] Solvent effects, accounted with the SMD implicit model,[63] were found to be particularly important for anionic and cationic reactions, but have a much smaller effect on radical reactivity.[§§]

The reactivity of [1.1.1]propellane with anions

Having identified the beneficial role of σ-π-delocalization and a suitable computational methodology, we set out to explore the reactivity of **1** under a variety of conditions. This began with a study of anion addition, for which a number of examples of have been reported to access aryl-, alkyl- and amino-substituted BCPs.[21–25] For instance, the Baran group described the addition of turbo-Hauser amides (R_2NMgCl•LiCl, R = alkyl) to form 1-amino-BCPs (Figure 3).[22] Given the apparent strain relief associated with this chemistry, it is somewhat surprising that extended reaction times (~16 h) and elevated temperatures (>50 °C) are often required. Walsh *et al.* studied the related addition of dithiane anions under similar conditions,[25] complementing their synthetic work with DFT calculations at the M06-2X level of theory,[64] which revealed carbanion addition to be highly endergonic. These examples led us to question the role of strain relief in the reaction of anions with **1**, in particular how a thermodynamically disfavored process could occur in a system thought to be primed to react.

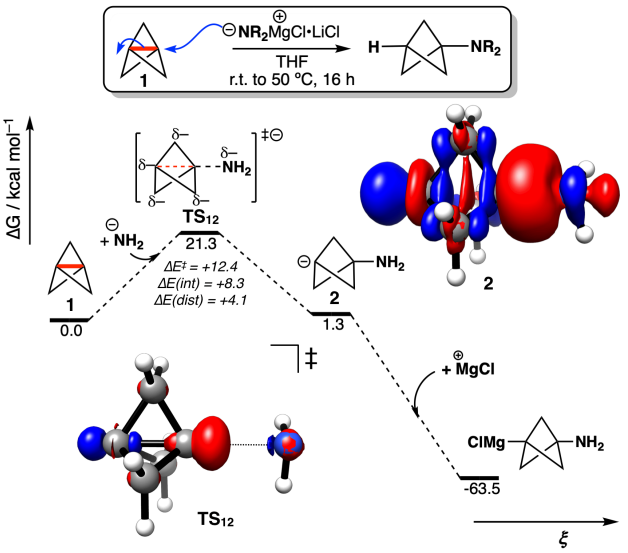

Figure 3. Reaction free energy profile for turbo-Hauser amide addition to **1**, calculated at SMD(THF)-DLPNO-CCSD(T)/ma-def2-QZVPP//SMD(THF)-B2GP-PLYP-D3BJ/ma-def2-TZVP. Electron density difference plots calculated at SMD(THF)-DLPNO-CCSD(T)/ma-def2-QZVPP; isovalue = 0.01 a.u.

The reaction of **1** with amide anions was computed using NH_2^- (Figure 3).[22] The formation of the BCP anion adduct **2** was found to be reversible and endergonic ($\Delta G^‡$ = 21.3 kcal mol^{-1}, ΔG = +1.3 kcal mol^{-1}); only on complexation of this species to a $MgCl^+$ ion did the overall reaction become highly exergonic (ΔG = –64.8 kcal mol^{-1}). To investigate the origin of the large energetic barrier to addition, a Distortion / Interaction Analysis (DIA) was performed,[30–32]

which separates the overall energy of the addition [ΔE(total)] into geometric distortion [ΔE(dist)] and electronic interactions [ΔE(int)] of the approaching species. Upon going from the reactant state to the transition state (TS), both ΔE(dist) and ΔE(int) were found to be positive, with ΔE(int) around twice the magnitude of ΔE(dist) (+8.3 and +4.1 kcal mol^{-1} respectively). This is highly unusual: To our knowledge, ΔE(int) has not been observed to be positive and greater than ΔE(dist) for any other system.[30]

Examination of the change in the geometry of the cage along the reaction coordinate reveals that distortion only occurs *after* the transition state (Figure S24), which suggests that strain relief alone is not responsible for the reactivity of **1**. Electron density difference analysis (EDDA) reveals that at the TS, electron density is pushed towards the back of the propellane cage (Figure 3, **TS12**, blue lobe). This correlates to a polarization of the delocalized electron density on addition of two electrons into the system from the nucleophile, which increases Pauli repulsion inside the cage. After the TS, the observation of extensive σ-π-delocalization (**2**) explains the now favorable interaction energy of the fragments. To maximize σ-π-delocalization, the cage is laterally compressed to increase the overlap of each wing carbon p orbital with the C1–C3 σ-antibonding orbital. This description is consistent with the relatively harsh reaction conditions often required for anionic additions, as significant electronic repulsion must be overcome prior to the development of the stabilizing σ-π-delocalization.

The reactivity of [1.1.1]propellane with radicals

Our attention next turned to the reactivity of **1** with radicals, chemistry that is of much utility in the synthesis of highly-functionalized BCPs.[15–19,28] Such reactions proceed through addition of a radical to the C1–C3, giving a BCP radical that subsequently reacts either via atom transfer, or addition to a radical trap (such as an azodicarboxylate, or a further molecule of **1**). Alkoxycarbonyl, alkyl and aryl radical additions have been studied using DFT (B3LYP, M06-2X, ωB97X-D, B2PLYP)[58,59,64,65] by the Uchiyama group[15] and ourselves,[16,17] where the focus has lain on the fate of the bicyclo[1.1.1]pentyl radical.

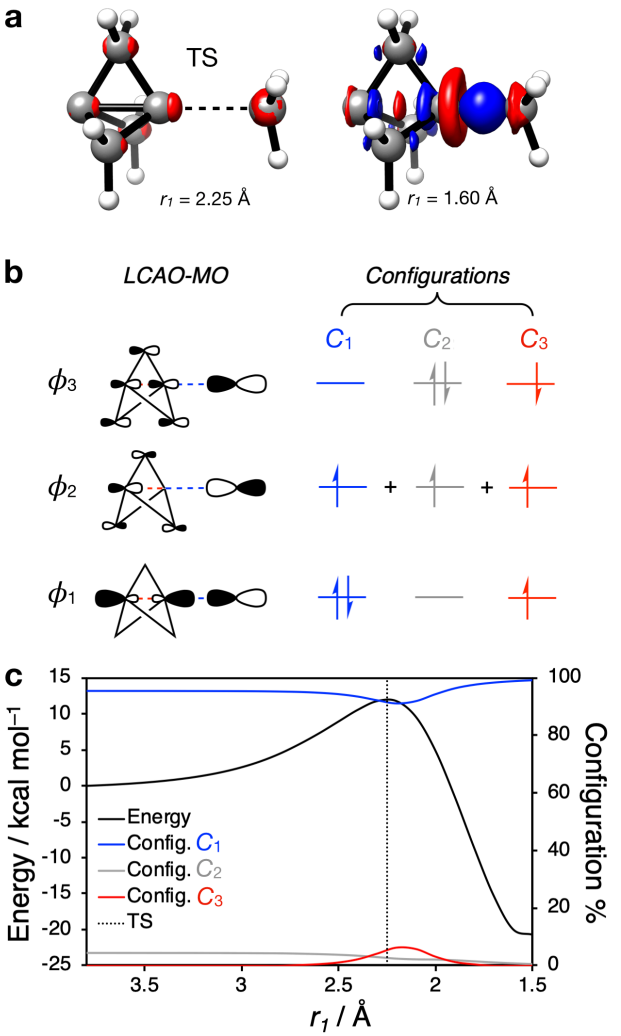

Figure 4. a. Electron density difference plot for the addition of $CH_3^{\bullet}$ to **1**, calculated at the [CASSCF(3,3)/def2-QZVPP] – [CASSCF(2,2)/def2-QZVPP + UHF/def2-QZVPP] level of theory for the adduct, **1** and methyl radical respectively; isovalue = 0.01 a.u. **b.** LCAO-MO depiction of the frontier molecular orbitals involved in the radical addition process to **1**, and the leading electronic configurations for the reaction. **c.** PES (CASSCF(3,3)/def2-QZVPP) for the addition of a methyl radical to **1**, showing the proportion of each leading electronic configuration as a function of the forming C–C bond (r_1).

We instead sought to study the initial radical addition to **1**, where a similar reactivity mode to the anionic addition was anticipated (Figure 4). The reaction pathway for the addition of $^{\bullet}CH_3$ reveals that the barrier to addition is once again dominated by ΔE(int), which can be rationalized through the injection of an electron into the system from the radical reactant (Figure S22). As in the anionic regime, ΔE(dist) only increases after the TS, suggesting that strain relief is not responsible for the reactivity profile. However, a subtle difference emerges between the radical and anionic reactivity modes: Due to the decreased electrostatic penalty in bringing two neutral species together compared with the anionic addition, charge is not expelled from the back of the cage (Figure 4a, r_1 = 2.25 Å). As a result, the additional electron density from the radical species must be incorporated *inside* the cage.

To understand how this repulsion could be overcome during the bond forming process, a linear combination of three atomic orbitals was constructed to form frontier MOs (LCAO-MO) for a CASSCF(3,3) calculation (Figure 4b, left). At large separation, these orbitals resemble those of the isolated species, with ϕ_1 and ϕ_3 corresponding to the HOMO and LUMO of **1** respectively (*vide supra*), and ϕ_2 corresponding to the p orbital of the radical species. Upon approach of the two species, the MOs mix such that ϕ_1 is the bonding combination, C_2 is non-bonding and ϕ_3 is the antibonding combination of the σ orbitals in the forming and breaking bonds. The electronic configurations C_i (Figure 4b, right) responsible for the population of these MOs changes over the course of the addition: While C_1 $[(\phi_1)^2(\phi_2)^1(\phi_3)^0]$ and C_2 $[(\phi_1)^0(\phi_2)^1(\phi_3)^2]$, corresponding to the HOMO-LUMO mixing in **1** itself, are dominant at large separations, the coefficients of these configurations decrease as the TS is approached (Figure 4c, blue and gray lines respectively). In their place, a new configuration C_3 $[(\phi_1)^1(\phi_2)^1(\phi_3)^1]$ emerges that corresponds to the singlet diradical state of **1** interacting with the approaching radical species (Figure 4b, red line); in essence, cleavage of the C1–C3 bond of **1** by a radical species requires access to an open-shell doublet electronic configuration. **1** itself is not diradicaloid in nature,[43] and as such a perturbation of the electronic structure of **1** by an approaching radical necessarily results in 'more diradical' configuration. This mixing of configurations coincides with the TS (Figure 4b, vertical dotted line), which correlates with the maximum repulsion that is the cause of the barrier to addition.

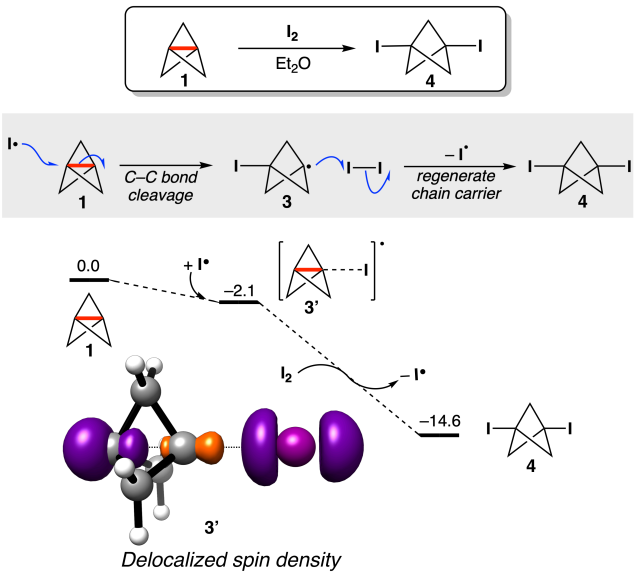

Figure 5. Proposed mechanism for the diiodination of **1** (top), and free energy profile for the diiodination of **1**, calculated at SMD(Et_2O)-DLPNO-CCSD(T)/def2-QZVPP//SMD(Et_2O)-B2GP-PLYP-D3BJ/def2-TZVP. Spin density of **3′** is plotted at an isovalue of 0.01 a.u.

In a similar manner to the anionic addition, the radical adduct is stabilized by σ-π-delocalization after the TS, which can be seen in Figure 4a (right) as blue lobes emanating from each wing carbon atom. However, given that the MO responsible for this σ-π-delocalization is only singly occupied, this effect is smaller in magnitude than in the anionic addition.

To test the consequences of this proposal in a chemically established setting, the diiodination of

1 was selected as a model reaction, not least given its utility as a method for the titration of solutions of **1** (Figure 5).[66] This reaction is reasonably presumed to occur via addition of I• to **1** to form an iodobicyclo[1.1.1]pentyl radical **3**, which is trapped by I_2 to afford 1,3-diiodoBCP **4**, regenerating I• as a chain carrier. However, computational study of this reaction revealed that the initial addition of I• did not proceed to the expected carbon-centered radical; remarkably, weak association of the iodine radical to **1** was favored over full C1–C3 bond cleavage, with only a slight increase in C–C bond length observed in **3'** compared with **1** (Δr_{C1-C3} = 0.02 Å).

This barrierless exergonic complexation (ΔG = – 2.1 kcal mol^{-1}) is followed by a barrierless atom transfer reaction with I_2. The observation of significant spin density delocalization in the radical adduct **3'** suggests that while the geometry of **1** is not significantly distorted, C1–C3 bond weakening nonetheless occurs to accommodate the unpaired electron, thus accounting for the ease of iodine atom abstraction from I_2 through the distal carbon atom. We propose that full C1–C3 cleavage does not occur because the formation of the C–I bond is not sufficient to outweigh the increase in Pauli repulsion in the bicyclopentyl radical adduct. Notably, the formation of this contact radical pair depends on the nature of the reacting radical X•; where a strong C–X bond would be formed upon addition, full cleavage of the inter-bridgehead C–C bond is seen (Figure S27). These results suggest that **1** has the potential to undergo reversible radical reactions, which again challenges the role of strain relief as a reaction driving force.

The reactivity of [1.1.1]propellane with cations

In both radical and anionic reactions, the propellane cage must accommodate an increase in electron density. This raised the question of the consequence of *removing* electrons from the cage, as would be expected in cationic activation. The reactions of **1** with cations is an underexplored field – despite the observation of rapid protonation by acetic acid,[26] no other cation-promoted reactions have been reported. Cationic bicyclo[1.1.1]pentyl adducts are known to rapidly fragment to bicyclo[1.1.0]butyl-1-carbinyl cations (Figure 6a),[67] which suggests a significant change in the electronics of the cage occurs as addition takes place.

EDDA on the model system of methyl cation addition to **1** indeed revealed contrasting behavior to that seen with anionic and radical additions. Instead of electron density being forced into the cage, charge transfer occurs upon approach of the cation to **1** (Figure 6b). No transition state is observed along the reaction coordinate (Figure 6c), which is consistent with the above discussion of the origins of transition state barriers for anionic and radical additions originating from the increase in electronic repulsion during the approach of the two species.

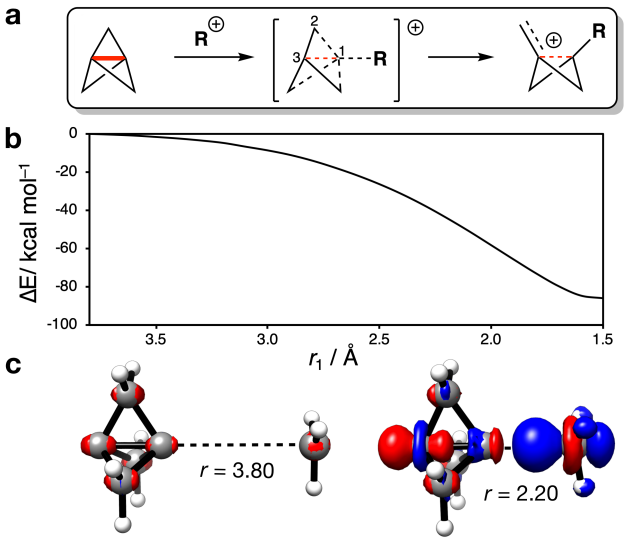

Figure 6. a. Addition of a cation to **1** results in cage fragmentation. **b.** PES for the addition of a methyl cation to **1**, calculated at SMD()-DLPNO-CCSD(T)/def2-QZVPP//CASSCF(2,3)/def2-QZVPP. **c.** Electron density difference calculated at [CASSCF(2,3)/def2-QZVPP] – [CASSCF(2,2)/def2-QZVPP + HF/def2-QZVPP] level of theory for the adduct, [1.1.1]propellane and methyl cation respectively; isovalue = 0.01 a.u.

Intriguingly, the C1–C3 bond was found to *decrease* in length over the course of the addition, which contrasts with the instinctive expectation that cationic addition should cleave (*i.e.* lengthen) this bond. This observation is in agreement with analogous observations by Jemmis and co-workers in calculations of halogen-bonded complexes of **1**, where the removal of electron density from the cage was suggested to *strengthen* the C1–C3 bond (B3LYP-D3BJ/QZ4P).[45] During reaction at C1, the frontside wing C1–C2 bonds lengthen, while the backside wing C3–C2 bonds shorten. The end result of this process is cleavage of *one* C1–C2 bond, forming a non-classical bicyclo[1.1.0]butyl-1-carbinyl cation. Within the framework of the highly-delocalized ground state of **1**, we suggest that relief of Pauli repulsion inside the cage through charge transfer *destabilizes* the cage structure, as σ-π-delocalization is lost, resulting in cage fragmentation.

A unified model for [1.1.1]propellane reactivity

The above results provide a unified framework that explains the omniphilic reactivity of [1.1.1]propellane with anions, radicals and cations. Two distinct modes of reactivity are defined, with the main features summarized as follows:

1. The ***ground state*** structure of **1** is stabilized by mixing of the σ-bonding and σ-antibonding / π-bonding orbitals. This σ-π-delocalization occurs to relieve Pauli repulsion inside the cage (Figure 7). This moldable electron density allows **1** to engage with electron-rich, -deficient and open-shell species.
2. ***Anionic*** and ***radical additions*** to **1** involve an increase in electronic repulsion inside an already electron-rich cage, causing a barrier to addition. To offset this effect, stabilization of the adduct occurs through σ-π-delocalization of electron density over the cage, which is accompanied by relief of geometric strain.
3. ***Cationic additions*** are dominated by loss of electron density from the electron-rich cage through charge transfer. Despite the cost associated with geometric reorganization, this process is barrierless due to the reduction of Pauli repulsion. However, as mitigation of Pauli repulsion was also in part responsible for the structural integrity of the propellane cage, this loss of stabilization can result in spontaneous fragmentation to form a bicyclo[1.1.0]butyl-1-carbinyl cation.

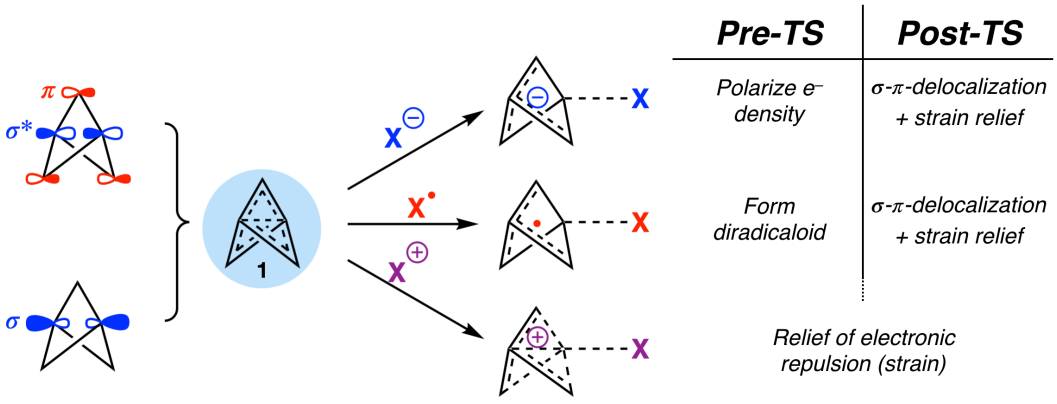

Figure 7. Summary of the omniphilic reactivity profile of **1**.

These generalized concepts should enable the development of new reactions of **1**, such as processes that capitalize on the unique structural distortion of the cage upon *loss* of electronic repulsion. We also predict that 'reversible addition' reactivity could feature in the formation of radical-pair complexes with species incapable of overcoming the delocalization energy of **1**. Moreover, we suggest that substitution of the apex carbon atoms, either as heteroatoms or with carbon-based substituents, will modify the degree of σ-π-delocalization both in the ground state and upon reaction. The effects of substitution on strain and electronic structure in [1.1.1]propellanes have been suggested to derive from changes in electronegativity; however, we propose that the ability of substituents to engage in σ-π-delocalization is an equally important effect to consider,[31,68,69] for example by stabilizing reaction pathways for addition reaction with electron-rich species by increased σ-π-delocalization.

Conclusions

The classical Lewis representation of [1.1.1]propellane places an inter-bridgehead bond along its central axis, which is thought to enable reactions through 'rapid strain relief'. Here, we have provided a unified framework that challenges this view, and explains the omniphilic reactivity profile of **1**. We show that the ground state electronic structure of **1** is best described as a delocalized electron density spanning the entire cage, originating from mixing of the inter-bridgehead C–C bonding and antibonding orbitals. The result is a moldable electron density that imparts a broad reactivity profile upon **1**: Anionic and radical additions are favored by stabilization of adducts through σ-π-delocalization, while reactions with cationic species are driven by charge transfer that relieves Pauli repulsion. We anticipate that this new understanding will open up possibilities for the exploration of novel reactivity of [1.1.1]propellane and related systems, and will provide a general framework to understand the behavior of strained cage-like molecules which continue to be of considerable interest in organic synthesis.

Conflicts of interest

There are no conflicts to declare.

Acknowledgements

We thank Prof. Sason Shaik and Prof. Philippe C. Hiberty for comments on the manuscript, and Prof. Igor V. Alabugin, Dr Alex J. W. Thom, Harry W. T. Morgan and Tom A. Young for insightful discussions. A.J.S. thanks the EPSRC Centre for Doctoral Training in Synthesis for Biology and Medicine for a studentship (EP/L015838/1), generously supported by AstraZeneca, Diamond Light Source, Defence Science and Technology Laboratory, Evotec, GlaxoSmithKline, Janssen, Novartis, Pfizer, Syngenta, Takeda, UCB and Vertex. A.J.S. also thanks the Oxford-Radcliffe Scholarship for a studentship. A.B.D. thanks the Heinrich Hertz Foundation for a fellowship. A.J.S. and F.D. thank the EPSRC Tier-2 National HPC Facility Service (http://www.cirrus.ac.uk), and the EPSRC Centre for Doctoral Training for Theory and Modelling in Chemical Sciences (EP/L015722/1) for providing access to the Dirac cluster at Oxford. E.A.A. thanks the EPSRC for support (EP/S013172/1).

Notes and references

§ Head-Gordon defines Pauli repulsion as "the marked increase in energy when two non-bonded atoms are forced to occupy the same space."[52] In the case of [1.1.1]propellane, the total kinetic energy of the electrons inside the cage increases as a result, destabilizing the molecule.[53]

§§ We should note that some single-hybrid functionals performed adequately to describe the kinetics of anionic addition; however, this occurs through fortuitous error cancellation, where small errors are observed in the activation barriers despite large errors in the density. Therefore, we cannot recommend their general use without a dedicated benchmarking study for each system.

(1) Levin, M. D., Kaszynski, P., Michl, J. "Bicyclo[1.1.1]pentanes, [n]Staffanes, [1.1.1]Propellanes, and Tricyclo[2.1.0.02,5]pentanes" *Chem. Rev.* **2000**, *100* (1), 169–234.

(2) Dilmaç, A. M., Spuling, E., de Meijere, A., Bräse, S. "Propellanes—From a Chemical Curiosity to 'Explosive' Materials and Natural Products" *Angew. Chem. Int. Ed.* **2017**, *56* (21), 5684–5718.

(3) Stepan, A. F., Subramanyam, C., Efremov, I. V., Dutra, J. K., O'Sullivan, T. J., Dirico, K. J., McDonald, W. S., Won, A., Dorff, P. H., Nolan, C. E., Becker, S. L., Pustilnik, L. R., Riddell, D. R., Kauffman, G. W., Kormos, B. L., Zhang, L., Lu, Y., Capetta, S. H., Green, M. E., Karki, K., Sibley, E., Atchison, K. P., Hallgren, A. J., Oborski, C. E., Robshaw, A. E., Sneed, B., and O'Donnell, C. J., "Application of the bicyclo[1.1.1]pentane motif as a nonclassical phenyl ring bioisostere in the design of a potent and orally active γ-secretase inhibitor" *J. Med. Chem.* **2012**, *55* (7), 3414–3424.

(4) Measom, N. D., Down, K. D., Hirst, D. J., Jamieson, C., Manas, E. S., Patel, V. K., Somers, D. O. "Investigation of a bicyclo[1.1.1]pentane as a phenyl replacement within an LpPLA2 Inhibitor" *ACS Med. Chem. Lett.* **2017**, *8* (1), 43–48.

(5) Auberson, Y. P., Brocklehurst, C. E., Furegati, M., Fessard, T. C., Koch, G., Decker, A., La Vecchia, L., Briard, E. "Improving Nonspecific Binding and Solubility: Bicycloalkyl Groups and Cubanes as para-Phenyl Bioisosteres" *ChemMedChem* **2017**, *12* (8), 590–598.

(6) Goh, Y. L., Cui, Y. T., Pendharkar, V., Adsool, V. A. "Toward Resolving the Resveratrol Conundrum: Synthesis and in Vivo Pharmacokinetic Evaluation of BCP-Resveratrol" *ACS Med. Chem. Lett.* **2017**, *8* (5), 516–520.

(7) Nicolaou, K. C., Vourloumis, D., Totokotsopoulos, S., Papakyriakou, A., Karsunky, H., Fernando, H., Gavrilyuk, J., Webb, D., Stepan, A. F. "Synthesis and Biopharmaceutical Evaluation of Imatinib Analogues Featuring Unusual Structural Motifs" *ChemMedChem* **2016**, *11* (1), 31–37.

(8) Wang, J., Lundberg, H., Asai, S., Martín-Acosta, P., Chen, J. S., Brown, S., Farrell, W., Dushin, R. G., O'Donnell, C. J., Ratnayake, A. S., Richardson, P., Liu, Z., Qin, T., Blackmond, D. G., and Baran, P. S., "Kinetically guided radical-based synthesis of C(sp3)–C(sp3) linkages on DNA" *Proc. Natl. Acad. Sci.* **2018**, *115* (28), E6404–E6410.

(9) Makarov, I. S., Brocklehurst, C. E., Karaghiosoff, K., Koch, G., Knochel, P. "Synthesis of Bicyclo[1.1.1]pentane Bioisosteres of Internal Alkynes and para-Disubstituted Benzenes from [1.1.1]Propellane" *Angew. Chem. Int. Ed.* **2017**, *56* (41), 12774–12777.

(10) Westphal, M. V., Wolfstädter, B. T., Plancher, J. M., Gatfield, J., Carreira, E. M. "Evaluation of tert-butyl isosteres: Case studies of physicochemical and pharmacokinetic properties, efficacies, and activities" *ChemMedChem* **2015**, *10* (3), 461–469.

(11) Itzhaki, L., Altus, E., Basch, H., Hoz, S. "Harder than diamond: Determining the cross-sectional area and Young's modulus of molecular rods" *Angew. Chem. Int. Ed.* **2005**, *44* (45), 7432–7435.

(12) Schwab, P. F. H., Noll, B. C., Michl, J. "Synthesis and structure of trigonal and tetragonal connectors for a 'Tinkertoy' construction set" *J. Org. Chem.* **2002**, *67* (16), 5476–5485.

(13) De Meijere, A., Messner, M. "Liquid Crystalline Bicyclo[1.1.1]pentane Derivatives" *Mol. Cryst. Liq. Cryst.* **1994**, *257* (1), 161–167.

(14) De Meijere, A., Ligang, Z., Belov, V. N., Bossi, M., Noltemeyer, M., Hell, S. W. "1,3-bicyclo[1.1.1]pentanediyl: The

shortest rigid linear connector of phenylated photochromic units and a 1,5-dimethoxy-9,10-di(phenylethynyl) anthracene fluorophore" *Chem. - A Eur. J.* **2007**, *13* (9), 2503–2516.

(15) Kanazawa, J., Maeda, K., Uchiyama, M. "Radical Multicomponent Carboamination of [1.1.1]Propellane" *J. Am. Chem. Soc.* **2017**, *139* (49), 17791–17794.

(16) Caputo, D. F. J., Arroniz, C., Dürr, A., Mousseau, J. J., Stepan, A. F., Mansfield, S. J., Anderson, E. A. "Synthesis and Applications of Highly Functionalized 1-Halo-3-Substituted Bicyclo[1.1.1]pentanes" *Chem. Sci.* **2018**, *9*, 5295–5300.

(17) Nugent, J., Arroniz, C., Shire, B. R., Sterling, A. J., Pickford, H. D., Wong, M. L. J., Mansfield, S. J., Caputo, D. F. J., Owen, B., Mousseau, J. J., Duarte, F. and Anderson, E. A., "A General Route to Bicyclo[1.1.1]pentanes through Photoredox Catalysis" *ACS Catal.* **2019**, *9* (10), 9568–9574.

(18) Bär, R. M., Kirschner, S., Nieger, M., Bräse, S. "Alkyl and Aryl Thiol Addition to [1.1.1]Propellane: Scope and Limitations of a Fast Conjugation Reaction" *Chem. - A Eur. J.* **2018**, *24* (6), 1373–1382.

(19) Kaszynski, P., Friedli, A. C., Michl, J. "Toward a Molecular-Size 'Tinkertoy' Construction Set. Preparation of Terminally Functionalized [n]Staffanes from [1.1.1]Propellane" *J. Am. Chem. Soc.* **1992**, *114* (2), 601–620.

(20) Bunker, K. D. "Propellane Derivatives and Synthesis" US2017081295, 2015.

(21) Messner, M., Kozhushkov, S. I., De Meijere, A. "Nickel- and palladium-catalyzed cross-coupling reactions at the bridgehead of bicyclo[1.1.1]pentane derivatives - A convenient access to liquid crystalline compounds containing bicyclo[1.1.1]pentane moieties" *Eur. J. Org. Chem.* **2000**, No. 7, 1137–1155.

(22) Gianatassio, R., Lopchuk, J. M., Wang, J., Pan, C.-M., Malins, L. R., Prieto, L., Brandt, T. A., Collins, M. R., Gallego, G. M., Sach, N. W., Spangler, J. E., Zhu, H., Zhu, J., and Baran, P. S., "Strain-release amination" *Science* **2016**, *351* (6270), 241–246.

(23) Lopchuk, J. M., Fjelbye, K., Kawamata, Y., Malins, L. R., Pan, C. M., Gianatassio, R., Wang, J., Prieto, L., Bradow, J., Brandt, T. A., Collins, M. R., Elleraas, J., Ewanicki, J., Farrell, W., Fadeyi, O. O., Gallego, G. M., Mousseau, J. J., Oliver, R., Sach, N. W., Smith, J. K., Spangler, J. E., Zhu, H., Zhu, J., and Baran, P. S., "Strain-Release Heteroatom Functionalization: Development, Scope, and Stereospecificity" *J. Am. Chem. Soc.* **2017**, *139* (8), 3209–3226.

(24) Shelp, R. A., Walsh, P. J. "Synthesis of BCP Benzylamines From 2-Azaallyl Anions and [1.1.1]Propellane" *Angew. Chem. Int. Ed.* **2018**, *57* (48), 15857–15861.

(25) Trongsiriwat, N., Pu, Y., Nieves-Quinones, Y., Shelp, R. A., Kozlowski, M. C., Walsh, P. J. "Reactions of 2-Aryl-1,3-Dithianes and [1.1.1]Propellane" *Angew. Chemie Int. Ed.* **2019**, *58*, 12416–13420.

(26) Wiberg, K. B., Dailey, W. P., Walker, F. H., Waddell, S. T., Crocker, L. S., Newton, M. D. "Vibrational Spectrum, Structure, and Energy of [1.1.1]Propellane" *J. Am. Chem. Soc.* **1985**, *107* (25), 7247–7257.

(27) Milligan, J. A., Wipf, P. "Straining to react" *Nat. Chem.* **2016**, *8*, 296–297.

(28) Wiberg, K. B., Waddell, S. T. "Reactions of [1.1.1]Propellane" *J. Am. Chem. Soc.* **1990**, *112* (6), 2194–2216.

(29) Wiberg, K. B. "The Concept of Strain in Organic Chemistry" *Angew. Chemie Int. Ed. English* **1986**, *25* (4), 312–322.

(30) Bickelhaupt, F. M., Houk, K. N. "Analyzing Reaction Rates with the Distortion/Interaction-Activation Strain Model" *Angew. Chem. Int. Ed.* **2017**, *56* (34), 10070–10086.

(31) Bickelhaupt, F. M. "Understanding reactivity with Kohn-Sham molecular orbital theory: E2-SN2 mechanistic spectrum and other concepts" *J. Comput. Chem.* **1999**, *20* (1), 114–128.

(32) Ess, D. H., Houk, K. N. "Theory of 1,3-dipolar cycloadditions: Distortion/interaction and frontier

molecular orbital models" *J. Am. Chem. Soc.* **2008**, *130* (31), 10187–10198.
(33) Seiler, P. "The Crystal Structure of [1.1.1]Propellane at 138 K" *Helv. Chim. Acta* **1990**, *73*, 1574–1585.
(34) Hedberg, L., Hedberg, K. "The Molecular Structure of Gaseous [1.1.1]Propellane: An Electron-Diffraction Investigation" *J. Am. Chem. Soc.* **1985**, *107* (25), 7257–7260.
(35) Harmony, M. D. "The equilibrium carbon-carbon single-bond length in ethane" *J. Chem. Phys.* **1990**, *93* (10), 7522–7523.
(36) Wiberg, K. B., Walker, F. H. "[1.1.1]Propellane" *J. Am. Chem. Soc.* **1982**, *104* (19), 5239–5240.
(37) Wiberg, K. B., Bader, R. F., Lau, C. D. "Theoretical Analysis of Hydrocarbon Properties. 1. Bonds, Structures, Charge Concentrations, and Charge Relaxations" *J. Am. Chem. Soc.* **1987**, *109* (4), 985–1001.
(38) Feller, D., Davidson, E. R. "Ab Initio Studies of [1. 1.1]- and [2.2.2]Propellane" *J. Am. Chem. Soc.* **1987**, *109* (14), 4133–4139.
(39) Kar, T., Jug, K. "Origin of the bridge bond in [1,1,1]propellane" *Chem. Phys. Lett.* **1996**, *256*, 201–206.
(40) Jensen, J. O. "Vibrational frequencies and structural determination of [1.1.1]propellane" *J. Mol. Struct. THEOCHEM* **2004**, *673* (1–3), 51–58.
(41) Polo, V., Andres, J., Silvi, B. "New Insights on the Bridge Carbon–Carbon Bond in Propellanes: A Theoretical Study Based on the Analysis of the Electron Localization Function" *J. Comput. Chem.* **2007**, *28*, 857–864.
(42) Yang, Y. "Two-center two-electron covalent bonds with deficient bonding densities" *J. Phys. Chem. A* **2012**, *116* (41), 10150–10159.
(43) Ramos-Cordoba, E., Salvador, P. "Diradical character from the local spin analysis" *Phys. Chem. Chem. Phys.* **2014**, *16*, 9565–9571.
(44) Bremer, M., Untenecker, H., Gunchenko, P. A., Fokin, A. A., Schreiner, P. R. "Inverted Carbon Geometries: Challenges to Experiment and Theory" *J. Org. Chem.* **2015**, *80* (12), 6520–6524.
(45) Joy, J., Akhil, E., Jemmis, E. D. "Halogen bond shortens and strengthens the bridge bond of [1.1.1]propellane and the open form of [2.2.2]propellane" *Phys. Chem. Chem. Phys.* **2018**, *20* (40), 25792–25798.
(46) Laplaza, R., Contreras-garcia, J., Fuster, F. "The 'inverted Bonds' revisited. Analysis of 'in silico' models and of [1.1.1]Propellane using Orbital Forces" *Chem. - A Eur. J.* **2019**, DOI:10.1002/chem.201904910.
(47) Wu, W., Gu, J., Song, J., Shaik, S., Hiberty, P. C. "The inverted bond in [1.1.1]propellane is a charge-shift bond" *Angew. Chem. Int. Ed.* **2009**, *48* (8), 1407–1410.
(48) Seiler, P., Belzner, J., Bunz, U., Szeimies, G. "Crystal Structure and Electron-Density Distribution of Two [1.1.1] Propellane Derivatives at 81 K" *Helv. Chim. Acta* **1988**, *71* (8), 2100–2110.
(49) Messerschmidt, M., Scheins, S., Grubert, L., Pätzel, M., Szeimies, G., Paulmann, C., Luger, P. "Electron density and bonding at inverted carbon atoms: An experimental study of a [1.1.1]propellane derivative" *Angew. Chem. Int. Ed.* **2005**, *44* (25), 3925–3928.
(50) Müller, B., Bally, T., Pappas, R., Williams, F. "Spectroscopic and computational studies on the rearrangement of ionized [1.1.1]propellane and some of its valence isomers: The key role of vibronic coupling" *J. Am. Chem. Soc.* **2010**, *132* (41), 14649–14660.
(51) Honegger, E., Huber, H., Heilbronner, E., Dailey, W. P., Wiberg, K. B. "Photoelectron Spectrum of [1.1.1]Propellane: Evidence for a Nonbonding MO?" *J. Am. Chem. Soc.* **1985**, *107* (24), 7172–7174.
(52) Horn, P. R., Mao, Y., Head-Gordon, M. "Defining the contributions of permanent electrostatics, Pauli repulsion, and dispersion in density functional theory calculations of intermolecular interaction energies" *J. Chem. Phys.* **2016**, *144* (11).
(53) Shaik, S., Danovich, D., Galbraith, J. M., Braida, B., Wu, W., Hiberty, P. C.

"Charge-Shift Bonding: A New and Unique Form of Bonding" *Angew. Chemie Int. Ed.* **2019**, *75252*, 2–20.
(54) McNaught, A. D., Wilkinson, A. "IUPAC Compendium of Chemical Terminology" IUPAC: Oxford, UK, 1997.
(55) Kim, M. C., Sim, E., Burke, K. "Understanding and reducing errors in density functional calculations" *Phys. Rev. Lett.* **2013**, *111* (7), 073003.
(56) Becke, A. D. "Density-functional exchange approximation with correct asymptotic behaviour" *Phys. Rev. A* **1988**, *38* (6), 3098–3100.
(57) Lee, C., Yang, W., Parr, R. G. "Development of the Colic-Salvetti correlation-energy formula into a functional of the electron density" *Phys. Rev. B* **1988**, *37* (2), 785–789.
(58) Becke, A. D. "Thermochemistry. III. The role of exact exchange" *J. Chem. Phys.* **1993**, *98*, 5648–5652.
(59) Grimme, S. "Semiempirical hybrid density functional with perturbative second-order correlation" *J. Chem. Phys.* **2006**, *124*, 034108.
(60) Kozuch, S., Gruzman, D., Martin, J. M. L. "DSD-BLYP: A general purpose double hybrid density functional including spin component scaling and dispersion correction" *J. Phys. Chem. C* **2010**, *114* (48), 20801–20808.
(61) Weigend, F., Ahlrichs, R. "Balanced Basis Sets of Split Valence, Triple Zeta Valence and Quadruple Zeta Valence Quality for H to Rn: Design and Assessment of Accuracy." *Phys. Chem. Chem. Phys.* **2005**, *7* (18), 3297–3305.
(62) Liakos, D. G., Neese, F. "Is It Possible to Obtain Coupled Cluster Quality Energies at near Density Functional Theory Cost? Domain-Based Local Pair Natural Orbital Coupled Cluster vs Modern Density Functional Theory" *J. Chem. Theory Comput.* **2015**, *11* (9), 4054–4063.
(63) Marenich, A. V., Cramer, C. J., Truhlar, D. G. "Universal solvation model based on solute electron density and a contiuum model of the solvent defind by the bulk dielectric constant and atomic surface tensions" *J. Phys. Chem. B.* **2009**, *113*, 6378–6396.
(64) Zhao, Y., Truhlar, D. G. "The M06 suite of density functionals for main group thermochemistry, thermochemical kinetics, noncovalent interactions, excited states, and transition elements: Two new functionals and systematic testing of four M06-class functionals and 12 other function" *Theor. Chem. Acc.* **2008**, *120* (1–3), 215–241.
(65) Chai, J.-D., Head-Gordon, M. "Long-range corrected hybrid density functionals with damped atom–atom dispersion corrections" *Phys. Chem. Chem. Phys.* **2008**, *10* (44), 6615–6620.
(66) Mondanaro, K. R., Dailey, W. P. "[1.1.1]Propellane" *Org. Synth.* **1998**, *75*, 98.
(67) Wiberg, K. B., McMurdie, N. "Formation and Reactions of Bicyclo[1.1.1]pentyl-1 Cations" *J. Am. Chem. Soc.* **1994**, *116* (26), 11990–11998.
(68) Xu, H., Saebo, S., Pittman, C. U. "A coupled-cluster approach to the relative strains in [1.1.1]propellane, its derivatives and hetero[1.1.1]propellanes" *Mol. Phys.* **2012**, *110* (19–20), 2349–2357.
(69) Belzner, J., Szeimies, G. "Thermal rearrangement of some [1.1.1] propellanes" *Tetrahedron Lett.* **1986**, *27* (48), 5839–5842.